Synthetic seismograms for *SH* waves in anelastic transversely isotropic media*

Lawrence H. T. Le, E. S. Krebes and Gerardo E. Quiroga-Goode

ABSTRACT

Following the first principle procedure outlined by Buchen (1971a) and Borcherdt (1973), we describe the derivation of *SH* wave propagation in a homogeneous transversely isotropic linear viscoelastic (HTILV) solid. Plane *SH* wave propagates with frequency-dependent complex phase velocity

$$\beta^2(\omega) = \beta_h^2(\omega)\ \sin^2 b + \beta_v^2(\omega)\ \cos^2 b$$

where β_h and β_v are complex shear wave velocities perpendicular and parallel to the axis of symmetry of the medium and b is a complex angle that the complex wavevector makes with the axis. The energy flows in a direction governed by the propagation vector, attenuation vector and the rigidities. The attenuation angle between the propagation vector and the attenuation vector can be uniquely determined by the complex ray parameter at the saddle point of the complex traveltime function. Complex ray can be traced between source and receiver locations with intermediate coordinates being complex. By means of the method of steepest descent, the wavenumber integral representing the exact *SH* wave field generated by a line source for layered-case problem can be approximated to give complex ray amplitudes for reflected and transmitted body waves. The factor accounting for cylindrical divergence is similar in form to that of the isotropic case. However, the similarity is not so obvious without going through the mathematics.

For a simple two half-spaces model, the complex ray result agrees well with the ω-k solution in regions away from the critical area. For pure *SH* mode propagation through a planar HTILV structure with 20% anisotropy, the reflected amplitudes in both cases (transversely isotropic and isotropic) look similar. However, the most significant is the kinematic difference.

INTRODUCTION

It is common observation that seismic waves propagating through the earth experience attenuation and dispersion. Besides anelasticity, anisotropy is an intrinsic property of the uppermost mantle accounting for the discrepancy of the Love- and Rayleigh-wave data (Anderson, 1989). Depending on the nature of anisotropy of the medium, the characteristics of seismic waves would be modified significantly and shear-waves splitting might occur (Tatham and McCormack , 1991).

* to be submitted to *Geophysical Journal International*.

A laminated solid appears to be transversely isotropic for waves whose wavelength is large compared to the layer thicknesses. Medium with transverse isotropy is very common in many sedimentary basins where layers of sand and shale are alternately deposited with thicknesses being small compared to the probing seismic wavelength. Previous works (i.e, De Segonzac and Laherrere, 1959) indicate that computation using either vertical velocities from sonic measurements or horizontal velocities from refraction surveys tend to give an underestimated or overestimated velocity-versus-depth model. Le (1992) has recently studied the case of *SH* wave propagating in two transversely isotropic half-spaces and found that the effect on seismic waves is not negligible.

In this paper, we extend the study of *SH* wave propagating in transversely isotropic and elastic medium by Sato and Lapwood (1968) to transversely isotropic linear viscoelastic medium in the framework of inhomogeneous wave theory (Buchen, 1971a; Borcherdt, 1973; Krebes and Hron, 1980). Daley and Hron (1979) studied the elastic case for a point source using asymptotic ray theory. Here, we focus on a simpler case of a line source. The purpose of this paper is twofold: (1) to provide a theoretical description of the solution and (2) to demonstrate the accuracy of the complex ray method for simple half-space model.

SH WAVES IN TRANSVERSELY ISOTROPIC LINEAR VISCOELASTIC MEDIA

The governing equation for the propagation of *SH* waves in a homogeneous transversely isotropic linear viscoelastic (HTILV) free space is

$$\rho \frac{\partial^2 u}{\partial t^2} = \frac{\partial \tau_{yx}}{\partial x} + \frac{\partial \tau_{yz}}{\partial z} \tag{1}$$

where u is the displacement with the corresponding Hooke's law :

$$\tau_{yx} = N(t) * d\left(\frac{\partial u}{\partial x}\right) \quad \text{and} \quad \tau_{yz} = L(t) * d\left(\frac{\partial u}{\partial z}\right) \tag{2}$$

where N and L are the elastic constants which are time-dependent, the (*) denotes the convolution operation

$$f * dg = \int_{-\infty}^{t} f(t-\tau)\, \dot{g}(\tau)\, d\tau \tag{3}$$

and the dot refers to the derivative with respect to the argument. In eq. (1), we have essentially assumed that *SH* wave particle motion is linear and in the *y*-direction. This is acceptable since it has been shown to be true for both a HILV medium (Borcherdt, 1977) and an elastic TI medium (Sato and Lapwood, 1968) separately. We could also have demonstrated it directly by generalizing the approach of Sato and Lapwood to a LV medium by replacing their products with convolutions [as in eq. (2)].

Substituting eq. (2) into (1) gives

$$\rho \frac{\partial^2 u}{\partial t^2} = N(t) * d\left(\frac{\partial^2 u}{\partial x^2}\right) + L(t) * d\left(\frac{\partial^2 u}{\partial z^2}\right) \tag{4}$$

in Cartesian coordinates. Taking Fourier transform, we get

$$-\rho\, \omega^2 \overline{u} = \widetilde{N}(\omega) \frac{\partial^2 \overline{u}}{\partial x^2} + \widetilde{L}(\omega) \frac{\partial^2 \overline{u}}{\partial z^2} \tag{5}$$

where

$$\overline{u}(\omega) = \int_{-\infty}^{\infty} u \; \exp(-i\, \omega\, t)\, dt \tag{6}$$

$$\widetilde{N}(\omega) = i\, \omega \int_0^{\infty} N(t) \exp(-i\, \omega\, t)\, dt \tag{7}$$

and

$$\widetilde{L}(\omega) = i\, \omega \int_0^{\infty} L(t) \exp(-i\, \omega\, t)\, dt \quad . \tag{8}$$

Consider a plane wave solution of the form

$$\overline{u} = \exp(-i\, \vec{K} \cdot \vec{x}) = \exp\left[-i\left(k_x\, x + k_z\, z\right)\right] \tag{9}$$

where the wavevector $\vec{K}$ is complex. By inserting equation (9) into (5), we obtain the dispersion relation

$$\rho\, \omega^2 = \widetilde{N}(\omega)\, k_x^2 + \widetilde{L}(\omega)\, k_z^2 \quad . \tag{10}$$

If we denote

$$\tan b = \frac{k_x}{k_z} \tag{11}$$

where b is a complex angle that $\vec{K}$ makes with the vertical axis of symmetry of the medium (see Hearn and Krebes, 1990 and Figure 1A), the complex phase velocity is given by

$$\beta^2(b) = \frac{\omega^2}{K^2} = \frac{\widetilde{N}\sin^2 b + \widetilde{L}\cos^2 b}{\rho} \tag{12}$$

or

$$\beta^2(b) = \beta_h^2 \sin^2 b + \beta_v^2 \cos^2 b \tag{13}$$

where the complex horizontal and vertical phase velocities, β_h and β_v are respectively :

$$\beta_h = \sqrt{\frac{\widetilde{N}}{\rho}} \quad \text{and} \quad \beta_v = \sqrt{\frac{\widetilde{L}}{\rho}} \quad . \tag{14}$$

Note that if the medium is elastic then $\widetilde{N}(\omega) = N$ and $\widetilde{L}(\omega) = L$ where N and L are constant. If we further write

$$\vec{K} = \vec{P} - i\,\vec{A} \tag{15}$$

then

$$K^2 = \vec{K}\cdot\vec{K} = \frac{\omega^2}{\beta^2} = P^2 - A^2 - 2i\,\vec{P}\cdot\vec{A} \tag{16}$$

where

$$\vec{P}\cdot\vec{A} = P\,A\cos\gamma \quad . \tag{17}$$

$\vec{P}$ is the (real) phase vector perpendicular to the planes of constant phase defined by $\vec{P}\cdot\vec{x} =$ constant, $\vec{A}$ is the (real) attenuation vector perpendicular to the planes of constant amplitude defined by $\vec{A}\cdot\vec{x} =$ constant and γ is the attenuation angle between $\vec{P}$ and $\vec{A}$ (see Figure 1B). Then, for a wave traveling in the positive x and z directions,

$$\vec{P} = \mathrm{Re}\,(k_x)\,\hat{x} + \mathrm{Re}\,(k_z)\,\hat{z} \quad , \tag{18}$$

$$\vec{A} = -\operatorname{Im}(k_x)\hat{x} - \operatorname{Im}(k_z)\hat{z} \quad , \tag{19}$$

and

$$\tan\theta = \frac{P_x}{P_z} \tag{20}$$

where $\hat{x}$ and $\hat{z}$ are the real unit Cartesian vectors in the x- and z-directions, Re(...) and Im(...) are the real and imaginary parts of a complex quantity and θ is the real angle that $\vec{P}$ makes with the vertical axis (Figure 1A and B). The complex ray parameter, p is given by

$$p = \frac{k_x}{\omega} = \frac{P_x - i\,A_x}{\omega} = \frac{\sin b}{\beta} \quad . \tag{21}$$

The components of the complex wave vector $\vec{K}$ are given in terms of p as:

$$k_x = \omega\, p \qquad \text{and} \qquad k_z = \omega\, \frac{\beta_h}{\beta_v}\sqrt{\frac{1}{\beta_h^2} - p^2} \quad . \tag{22}$$

Hence, if the frequency-dependent phase velocities, β_h and β_v and a value of p are given, the phase vector, $\vec{P}$ and the attenuation vector, $\vec{A}$ can be obtained via (22).

Here we compute the energy flux for *SH* wave in HTILV solid. Consider a *SH* plane wave propagating in the x-z plane with displacement

$$u = D\, \exp\left[i\left(\omega t - \vec{K}\cdot\vec{x}\right)\right] \tag{23}$$

where D is a complex constant. The energy propagates in a direction specified by the energy flux vector

$$\langle \vec{I} \rangle = \left(-\langle (\tau_{xy})_R\, (\dot{u})_R \rangle , 0, -\langle (\tau_{zy})_R\, (\dot{u})_R \rangle \right) \tag{24}$$

$$= \frac{1}{2}\,\omega |D|^2\, e^{-2\vec{A}\cdot\vec{x}} \left[\operatorname{Re}\left(\tilde{N}\, K_x\right), 0, \operatorname{Re}\left(\tilde{L}\, K_z\right) \right]$$

$$= \frac{1}{2}\,\omega |D|^2\, e^{-2\vec{A}\cdot\vec{x}} \left[\left(\tilde{N}_R\, P_x + \tilde{N}_I\, A_x\right), 0, \left(\tilde{L}_R\, P_z + \tilde{L}_I\, A_z\right) \right] \tag{25}$$

where the subscripts, R or I denote the real or imaginary part of a complex quantity and $\langle \ldots \rangle$ denotes the time average. In the HTILV solid, the energy propagates along a direction which is neither $\vec{P}$ nor $\vec{A}$, just as for a HILV solid. In the absence of anelasticity of the medium (N and L are constant) and for the case of body waves, $\vec{A} = 0$ and eq. (25) reduces to

$$\langle \vec{I} \rangle = \frac{1}{2}\,\omega |D|^2 [\, N\ P_x , 0, L\, P_z \,]$$
$$= \frac{1}{2}\,\omega |D|^2 \left[\, N\ K \sin\theta , 0, L\, K \cos\theta \,\right]$$
$$= \frac{1}{2}\,\rho\,\omega^2 |D|^2 \left[\frac{\beta_h^2}{\beta} \sin\theta , 0, \frac{\beta_v^2}{\beta} \cos\theta \right] \tag{26}$$

where equations ((7), (8), (12), (14), (15) and (20) are employed and β, β_h and β_v are independent of frequency. The elastic ray velocity V is related to the elastic phase velocity β by

$$\beta(\theta) = V(\phi) \cos\left(\phi - \theta \right) \tag{27}$$

where ϕ is the ray angle which the ray makes with the z-axis (see Figure 1A and Byun, 1984) or

$$\beta\, V \cos\phi = \beta_v^2 \cos\theta \quad \text{and} \quad \beta\, V \sin\phi = \beta_h^2 \sin\theta \tag{28}$$

(Sato and Lapwood, 1968). By substituting (28) into (26), we obtain

$$\langle \vec{I} \rangle = \frac{1}{2}\,\rho\,\omega^2 |D|^2 \left[\, V \sin\phi , 0, V \cos\phi \,\right] \quad . \tag{29}$$

Thus, the disturbance propagates along the ray direction with a ray velocity V in the elastic *TI* solid (Sato and Lapwood, 1968).

COMPLEX RAY TRACING IN MEDIUM WITH ELLIPTICAL VELOCITY DEPENDENCY

For a harmonic plane wave

$$\exp \{ i\, \omega\, [t - T(\omega)] \} \tag{30}$$

traveling a displacement $\vec{x}$ from the origin to (x, z) in a homogeneous medium (see Figure 1A), the complex traveltime function is

$$T(p) = \frac{\vec{K} \cdot \vec{x}}{\omega} = px + \frac{\beta_h}{\beta_v} \sqrt{\frac{1}{\left(\beta_h^2\right)} - p^2} \; z \quad . \tag{31}$$

For a stack of flat homogeneous linear viscoelastic layers with elliptical velocity dependency, the complex traveltime function can be generalized as

$$T(p) = \sum_{j=1}^{m} \frac{\vec{K}_j \cdot \vec{x}_j}{\omega} = pX + \sum_{j=1}^{m} \frac{\left(\beta_h\right)_j}{\left(\beta_v\right)_j} \sqrt{\frac{1}{\left(\beta_h^2\right)_j} - p^2} \; h_j \tag{32}$$

where m is the number of ray segments, h_j is the thickness of the layer which the jth ray segment traverses, etc., and X is the total offset (Figure 2). Since the quantities, p, β_h and β_v are complex and dependent on frequency, Re(T) is the actual travel time of ray and Im(T) is associated with absorption.

Since the traveltime function $T(p)$ is determined if p is obtained, the unique value p_s of p for a given ray can be achieved by finding the stationary travel path, i.e., p_s is obtained from

$$\left. \frac{d\,T(p)}{dp} \right|_{p=p_s} = 0 \tag{33}$$

or

$$X = \sum_{j=1}^{m} \frac{h_j \, p_s \left(\beta_h\right)_j}{\left(\beta_v\right)_j \sqrt{\frac{1}{\left(\beta_h^2\right)_j} - p_s^2}} \quad . \tag{34}$$

This method has been called the stationary ray method and the ray the stationary ray satisfying Fermat's principle of least time (Hearn and Krebes, 1990).

If we define the angle ξ_j by

$$p = \frac{\sin \xi_j}{\left(\beta_h\right)_j} \quad , \quad j = 1, \ldots, m \tag{35}$$

then (34) becomes

$$X = \sum_{j=1}^{m} \frac{\left(\beta_h\right)_j}{\left(\beta_v\right)_j} h_j \tan\left(\xi_s\right)_j \tag{36}$$

where

$$\tan\left(\xi_s\right)_j = \frac{x_j}{\dfrac{\left(\beta_h\right)_j}{\left(\beta_v\right)_j} h_j} \tag{37}$$

and $\left(\xi_s\right)_j = \left[\xi(p_s)\right]_j$ is a complex auxiliary angle (see Figure 1A). Although each term in the sums in (34) or (36) is complex, the sum X is a real number. Substituting Equations (35) and (36) into (32) yields

$$T(p) = \sum_{j=1}^{m} \frac{h_j}{\left(\beta_v\,\beta_h\right)_j \sqrt{\dfrac{1}{\left(\beta_h^2\right)_j} - p_s^2}} = \sum_{j=1}^{m} \frac{s_j}{\left(\beta_h\right)_j} \quad . \tag{38}$$

where $s_j = \sqrt{x_j^2 + \left(\dfrac{\beta_h^2}{\beta_v^2}\right)_j h_j^2}$ is a complex stretched arc length.

For a given ray, p_s is obtained by solving eq. (34), given $\left[\beta_h(\omega)\right]_j$ and $\left[\beta_v(\omega)\right]_j$ (or $\widetilde{N}_j(\omega)$ and $\widetilde{L}_j(\omega)$). Another approach would be to use the (real) phase velocities of homogeneous waves in the horizontal and vertical directions, $[c_h(\omega)]_j$ and $[c_v(\omega)]_j$, and the Q-values in the horizontal and vertical directions, $[Q_h(\omega)]_j$ and $[Q_v(\omega)]_j$ as the given input values (see, e.g., Hearn and Krebes, 1990). In that case, $\left(\beta_h\right)_j$ can be obtained from

$$\frac{1}{\left(\beta_h\right)_j^2} = \frac{1}{\left(c_h\right)_j^2} \left\{ \frac{2\left[1 - i\,(Q_h)_j^{-1}\right]}{1 + \sqrt{\left[1 + (Q_h)_j^{-2}\right]}} \right\} \tag{39}$$

with a similar equation holding for $\left(\beta_v\right)_j$ (with "h" replaced by "v"), and where

$$(Q_h)_j^{-1} = \frac{\mathrm{Im}(\widetilde{N}_j)}{\mathrm{Re}(\widetilde{N}_j)} \quad \text{and} \quad (Q_v)_j^{-1} = \frac{\mathrm{Im}(\widetilde{L}_j)}{\mathrm{Re}(\widetilde{L}_j)} \quad . \tag{40}$$

RAY AMPLITUDES

The displacement due to an impinging *SH* ray of *m* segments from a line source passing through a sequence of flat HTILV layers (Figure 2) is (generalized from the elastic TI two half-spaces solution, Le, 1992 and using the elastic- viscoelastic correspondence principle), without a constant factor,

$$u = \int_{-\infty}^{\infty} \frac{F(\omega)\, S(\omega)}{i\,\rho_1 \left(\beta_v\right)_1^2}\, e^{\,i\,\omega t}\, d\,\omega \tag{41}$$

where

$$F(\omega) = \int_{-\infty}^{\infty} \frac{\Upsilon}{v_1} \exp\left[-i\,\omega\left(\sum_{j=1}^{m} v_j\, h_j + pX\right)\right] d\,p \quad , \tag{42}$$

$$v_j = \frac{\left(\beta_h\right)_j}{\left(\beta_v\right)_j} \sqrt{\frac{1}{\left(\beta_h\right)_j^2} - p^2} = \frac{\cos \xi_j}{\left(\beta_v\right)_j} \quad , \tag{43}$$

$S(\omega)$ is the spectrum of the source function and Υ is the product of anelastic and transversely isotropic generalized reflection coefficients $\Re$ and transmission coefficients Γ (Spencer, 1960; Krebes, 1984; Le, 1992):

$$\Upsilon = \prod_{j,\,l} \Re_{j-1,\,j}\; \Gamma_{l-1,\,l} \tag{44}$$

$$\Re_{j-1,\,j} = \frac{\widetilde{L}_{j-1} v_{j-1} - \widetilde{L}_j\, v_j}{\widetilde{L}_{j-1} v_{j-1} + \widetilde{L}_j\, v_j} \quad \text{and} \quad \Gamma_{j-1,\,j} = \frac{2\,\widetilde{L}_{j-1} v_{j-1}}{\widetilde{L}_{j-1} v_{j-1} + \widetilde{L}_j\, v_j} \quad . \tag{45}$$

For large and positive ω, the exact p–integral, $F(\omega)$ can be approximated by the method of steepest descent (Brekhovskikh, 1980):

$$F(\omega) = \sqrt{\frac{2\pi}{i\omega\, T''(p_s)}}\; \frac{\Upsilon(p_s)}{v_1(p_s)}\; \exp[\,-i\;\omega\, T(p_s)] \tag{46}$$

where $T(p)$ is given by (38) and the second derivative of $T(p)$ is

$$T''(p) = -\sum_{j=1}^{m} \frac{h_j \left(\beta_h\right)_j^2}{\left(\beta_v\right)_j \cos^3 \xi_j} \tag{47}$$

via (43). In obtaining eq. (46), we did not examine in detail the geometry of the p-plane, i.e., the location of the saddle point with respect to the branch cuts, how these vary with the medium parameters, etc. This is because we are interested here only in reflected and transmitted body waves, whose amplitudes are given by the saddle point contribution to the integral. The form of this contribution seems to be essentially independent of the above-mentioned details (see, e.g., Buchen, 1971b; Aki and Richards, 1980).

By substitution, we have

$$u = \sqrt{2\pi} \int_{-\infty}^{\infty} \sqrt{\frac{(\beta_h)_1}{\omega}} \frac{Y_s}{L_s} \frac{S(\omega)}{i\,\rho_1 (\beta_v)_1^2} \exp\left(i \left\{ \frac{\pi}{4} + \omega[t - T(p_s)] \right\}\right) d\,\omega \tag{48}$$

where the cylindrical geometrical spreading L_s is

$$L_s = \frac{(\beta_h)_1}{(\beta_v)_1} \cos(\xi_s)_1 \left(\frac{1}{(\beta_h)_1} \sum_{j=1}^{m} \frac{h_j (\beta_h)_j^2}{(\beta_v)_j \cos^3(\xi_s)_j} \right)^{1/2} . \tag{49}$$

In the case that the medium is homogeneous(meaning $m = 1$) and isotropic, the spreading factor L_s reduces to $\sqrt{length}$ of the ray as desired.

In eq. (48), a "high frequency" source pulse spectrum $S(w)$ should be used, since eq. (46) is a high frequency approximation. Also, the signs of the complex vertical slownesses v_j must be chosen correctly (see Richards, 1984; Krebes, 1984).

DISCUSSION OF THE NUMERICAL RESULTS

In this section, we compare synthetic seismograms generated by eq. (41), evaluated by the ω-k method of Abramovici et al. (1990), with those generated by the stationary ray method (eq. 48).

The source pulse we use is that of Abramovici et al. (1990), i.e., the time derivative of a delayed Gaussian function. The spectrum of this pulse is given by

$$S(\omega) = i\,\omega \sqrt{\frac{\pi}{\sigma}} \exp\left(-\frac{\omega^2}{4\sigma} - i\,\omega\,t_d\right) \tag{50}$$

where $\sigma = 5 \times 10^4$, the dominant radial frequency $\omega_d = \sqrt{2\sigma} \approx 2\pi \times 50$ Hz, and the time delay $t_d = \sqrt{2/\sigma}$ makes the pulse essentially causal.

The intrinsic absorption law we implemented is also that used by Abramovici et al. (1990), i.e., Azimi's law (Azimi et al., 1968; Aki and Richards, 1980), e.g.,

$$\beta_h(\omega) = \beta_{hr} \left[1 + \frac{1}{\pi Q_h} \ln\left(\frac{f}{f_r}\right) + \frac{i}{2Q_h} \right] \tag{51}$$

with a similar equation for β_v. The reference frequency $f_r = 0.1$ Hz. The velocity β_{hr} is found by assuming that $\mathrm{Re}\left[\beta_h(\omega)\right]$ approaches the model velocity at $f = 250$ Hz. Below the reference frequency, there is no dispersion, the elastic velocity being replaced by $\beta_{hr}(1 + i/2Q_h)$.

The medium model consists of two half spaces, with the source and receivers in the upper-space at a distance of 0.5 km above the interface. Using the subscript 1(2) to refer to the upper (lower) half-space, the densities are $\rho_1 = 1.5$ g/cm^3 and $\rho_2 = 2.0$ g/cm^3, the model velocities for the isotropic case are $\beta_1 = 1.0$ km/s and $\beta_2 = 2.0$ km/s, and the Q values are $Q_1 = 50$ and $Q_2 = 100$. For the case of transverse isotropy, we use $\beta_h/\beta_v = 1.2$ for the model velocity ratio in each half-space, with β_v being the model velocity for the isotropic case. Q-anisotropy was not considered, i.e., $Q_h = Q_v \equiv Q$.

Figures 3 and 4 show the synthetic seismograms for the anelastic isotropic and anelastic anisotropic cases. The head wave, which can be easily seen on the ω-k traces, is not computed in the stationary ray code. As expected, the ω-k and the stationary ray method agree quite well in the subcritical zone, disagree completely in the critical zone (a small range about the critical distance) due to the absence of the head wave in the ray method and the inaccuracy of ray theory in the critical zone, and agree fairly well in the supercritial zone. As expected, the waves in the anisotropic case arrive before those in the isotropic case, and this traveltime difference increases with offset, due to the higher horizontal velocity in the anisotropic case. Figure 5 shows the ray-synthetic results for the model given in TABLE 1 with β_v being the model velocity for the isotropic case. Again, Q-anisotropy is not considered. Four reflected events are displayed in four different windows for comparison purpose. The reflected amplitudes in both cases

ρ (g/cm^3)	β_v (km/s)	β_h (km/s)	Q	h (km)
2.0	1.80	2.16	40	∞
2.1	2.30	2.76	50	1.0
2.2	3.00	3.60	60	1.0
2.3	4.00	4.80	70	1.5
2.4	4.80	5.76	80	∞

TABLE 1 : The TI model with $\beta_h/\beta_v = 1.2$. The line source and the receivers are located in the upper half-space at a distance of 0.5 km above the first interface.

(transversely isotropic versus isotropic) are not much different, especially the later events. The reflection coefficients seem to be insensitive to the underlying anisotropy as discussed by Schoenberg and Costa (1991). However, the difference in arrival times is the most striking

CONCLUSION

A complete description of *SH* wave propagation in HTILV medium has been presented. The energy propagates along a direction dictated by the real phase vector, real attenuation vector and the real and imaginary part of the rigidities. The stationary ray can be traced through a sequence of HTILV layers by computing the saddle point value of the ray parameter. Full wave solution can be obtained by calculating the double integral given by equations (41) and (42). For body waves, the double integral can be approximately reduced to a single integral of (48) by means of the method of steepest descent.

For a simple model of two half-spaces, results computed by the two methods (the ω-k and the stationary ray method) compare well in the subcritical and the supercritical zones. For the multi-layered structure that we considered, transverse anisotropy does not seem to modify the reflection coefficients significantly; rather, the most obvious difference is the early arrival of the reflected events as compared to the isotropic results.

ACKNOWLEDGMENTS

This research was supported by the sponsors of the Consortium for Research in Elastic Wave Exploration Seismology (the CREWES project). We would like to thank Drs. Robert Stewart and Don Lawton for encouragement. G.E.G. wishes to express his gratitude to the Mexican funding authority, CONACYT for financial support.

REFERENCES

Aki, K., and P. G. Richards (1980). *Quantitative seismology,* W. H. Freeman and Company, San Francisco.

Anderson, D. L. (1989). *Theory of the Earth,* Blackwell Scientific Publications, Chapter 14.

Azimi S. A., Kalinin A.V., Kalinin V. V. and Pivovarov (1968). Impulse and transient characteristics of media with linear and quadratic absorption laws. *Izvestiya, Physics of the Solid Earth* **2**, 88-93.

Borcherdt, R. D. (1977). Reflection and refraction of type – II *S* waves in elastic and anelastic media, *Bull. Seism. Soc. Am.* **67**, 43-67.

Borcherdt, R. D. (1973). Energy and plane waves in linear viscoelastic media, *J. Geophys. Res.* **78**, 2442-2453.

Buchen, P. W. (1971a). Plane waves in linear viscoelastic media, *Geophys. J. R. Astr. Soc.* **23**, 531-542.

Buchen, P. W. (1971b). Reflection, transmission and diffraction of *SH*-waves in linear viscoelastic solids, *Geophys. J. R. Astr. Soc.* **25**, 97-113.

Brekhovskikh, L. M. (1980). *Waves in layered media,* Academic Press, New York.

Byun, B. S. (1984). Seismic parameters for transversely isotropic media, *Geophysics* **49**, 1908 - 1914.

Daley, P. F., and F. Hron (1980). *SH* waves in layered transversely isotropic media - an asymptotic expansion approach, *Bull. Seism. Soc. Am.* **69**, 689-711.

De Segonzac, P. D., and J. Laherrere (1959). Application of the continuous velocity log to anisotropy measurements in Northern Sahara; results and consequences, *Geophy. Prosp.* **7**, 202-217.

Hearn, D. J., and E. S. Krebes (1990). On computing ray-synthetic seismograms for anelastic media using complex rays, *Geophysics* **55**, 422-432.

Krebes, E. S. (1984). On the reflection and transmission of viscoelastic waves – some numerical results, *Geophysics* **49**, 1374-1380.

Krebes, E. S., and F. Hron (1980). Ray -synthetic seismograms for *SH* waves in anelastic media, *Bull. Seism. Soc. Am.* **70**, 29-46.

Le, L. H. T. (1992). On Cagniard's problem for an *qSH* line source in transversely–isotropic media, submitted to *Bull. Seism. Soc. Am.*.

Richards, P. G. (1980). On wavefronts and interfaces in anelastic media, *Bull. Seism. Soc. Am.* **74**, 2157-2165.

Sato, R., and E. R. Lapwood (1968). *SH* waves in transversely isotropic medium – I, *Geophys J. R. astr. Soc.* **14**, 463-470.

Spencer, T. W. (1960). The method of generalized reflection and transmission coefficients, *Geophysics* **25**, 625-641.

Schoenberg, M., and J. Costa (1991). The insensitivity of reflected *SH* waves to anisotropy in an underlying layered medium, *Geophy. Prosp.* **39**, 985-1003.

Tatham, R. H., and M. D. McCormack (1991). *Multicomponent seismology in petroleum exploration*, Society of exploration geophysicists, Chapter 2.

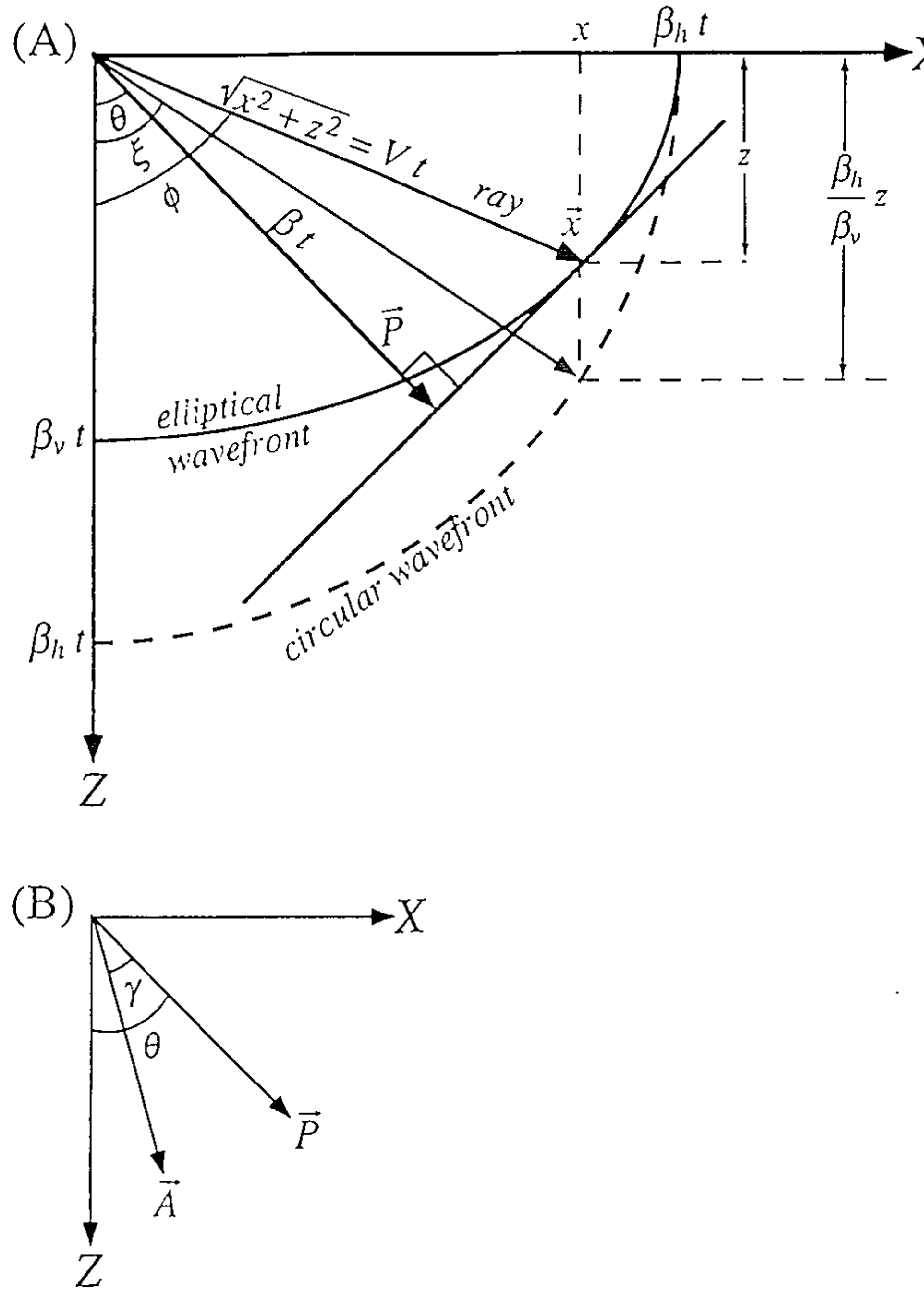

Figure 1. (A) A schematic diagram showing the phase vector, $\vec{P}$, $\vec{x}$, θ, ξ, ϕ and a ray for an elastic transversely isotropic whole space. Here we assume $\beta_v < \beta_h$. .The elliptical wavefront will approach the circular wavefront when $\beta_v \rightarrow \beta_h$ or the medium is more isotropic. In the case that the medium is anelastic, $\vec{P}$ is replaced by $\vec{K}$ and θ is replaced by b . (B) A diagram showing the phase vector, $\vec{P}$, the attenuation vector, $\vec{A}$ and the attenuation angle, γ in the anelastic case.

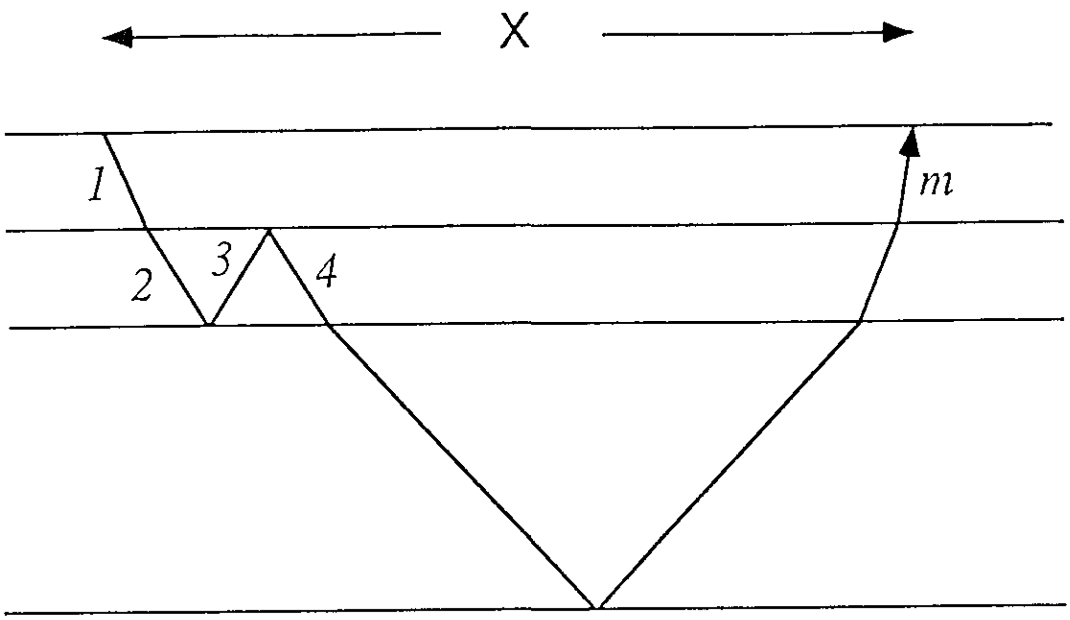

Figure 2. A ray of m segments.

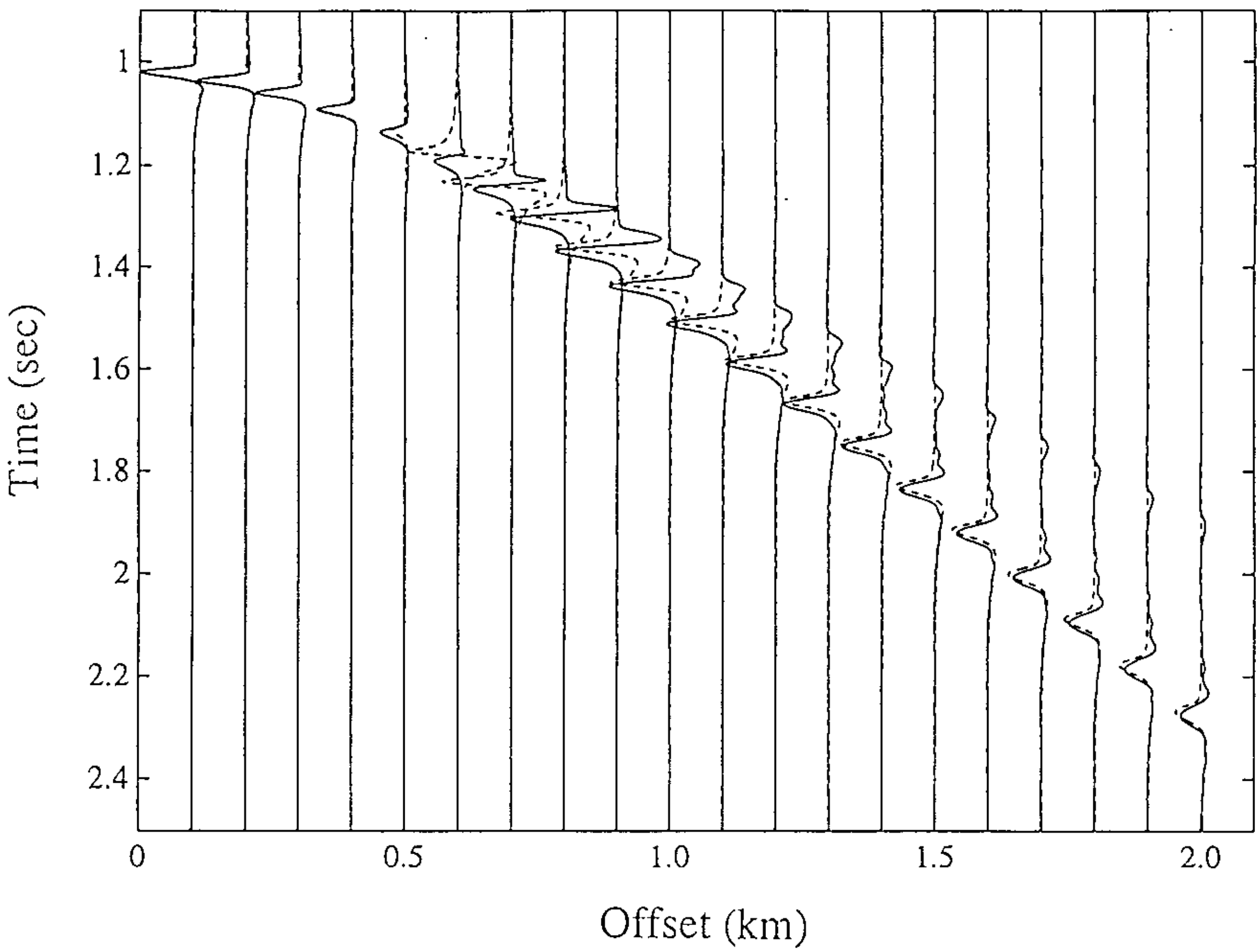

Figure 3. Synthetic seismograms for the medium model in the anelastic isotropic case (see text for model parameters). The solid line traces are computed by the ω-k method, and the dashed line traces by the stationary ray method.

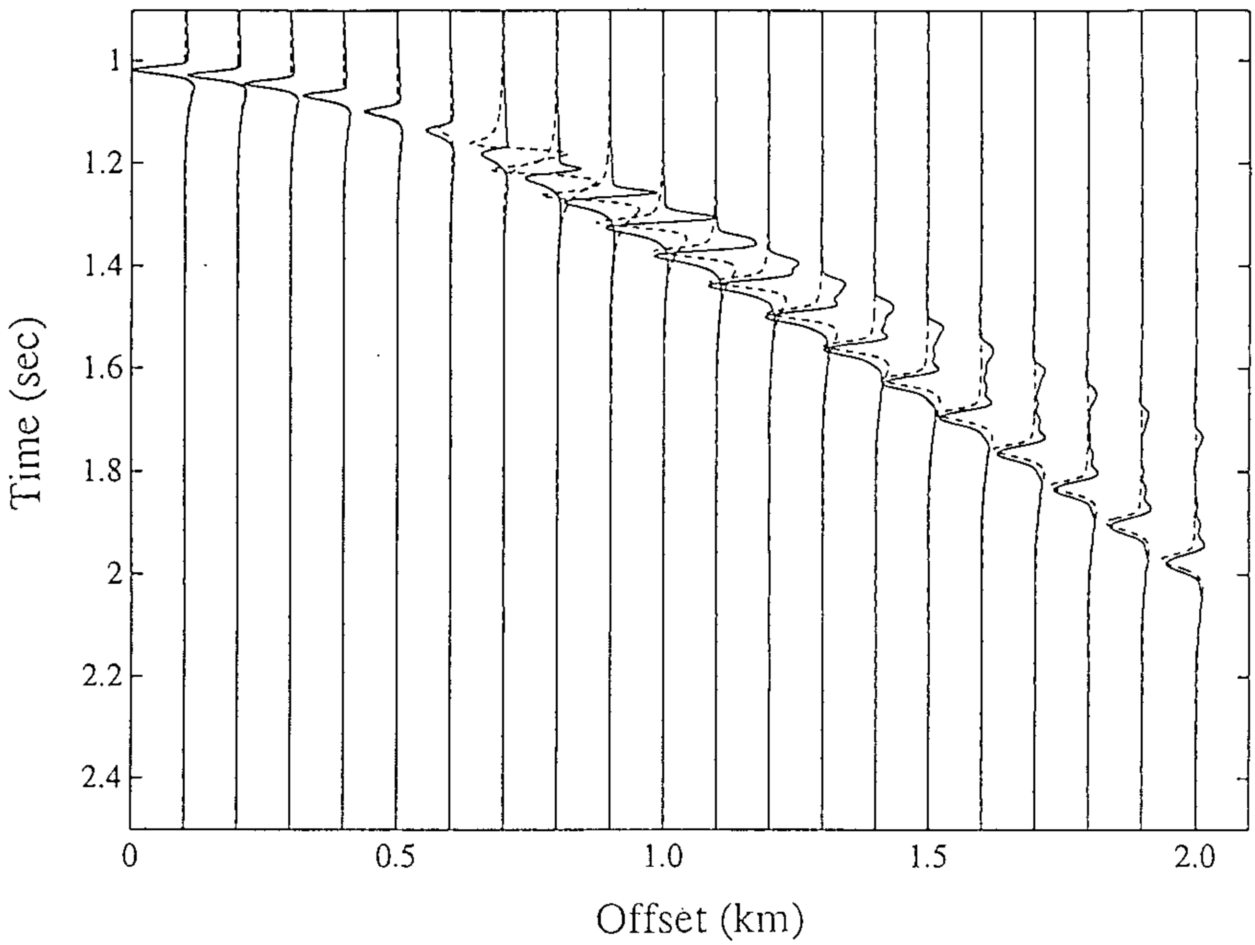

Figure 4. Synthetic seismograms for the medium model in the anelastic anisotropic case (see the text for model parameters). The solid line traces are computed by the ω-k method, and the dashed line traces by the stationary ray method.

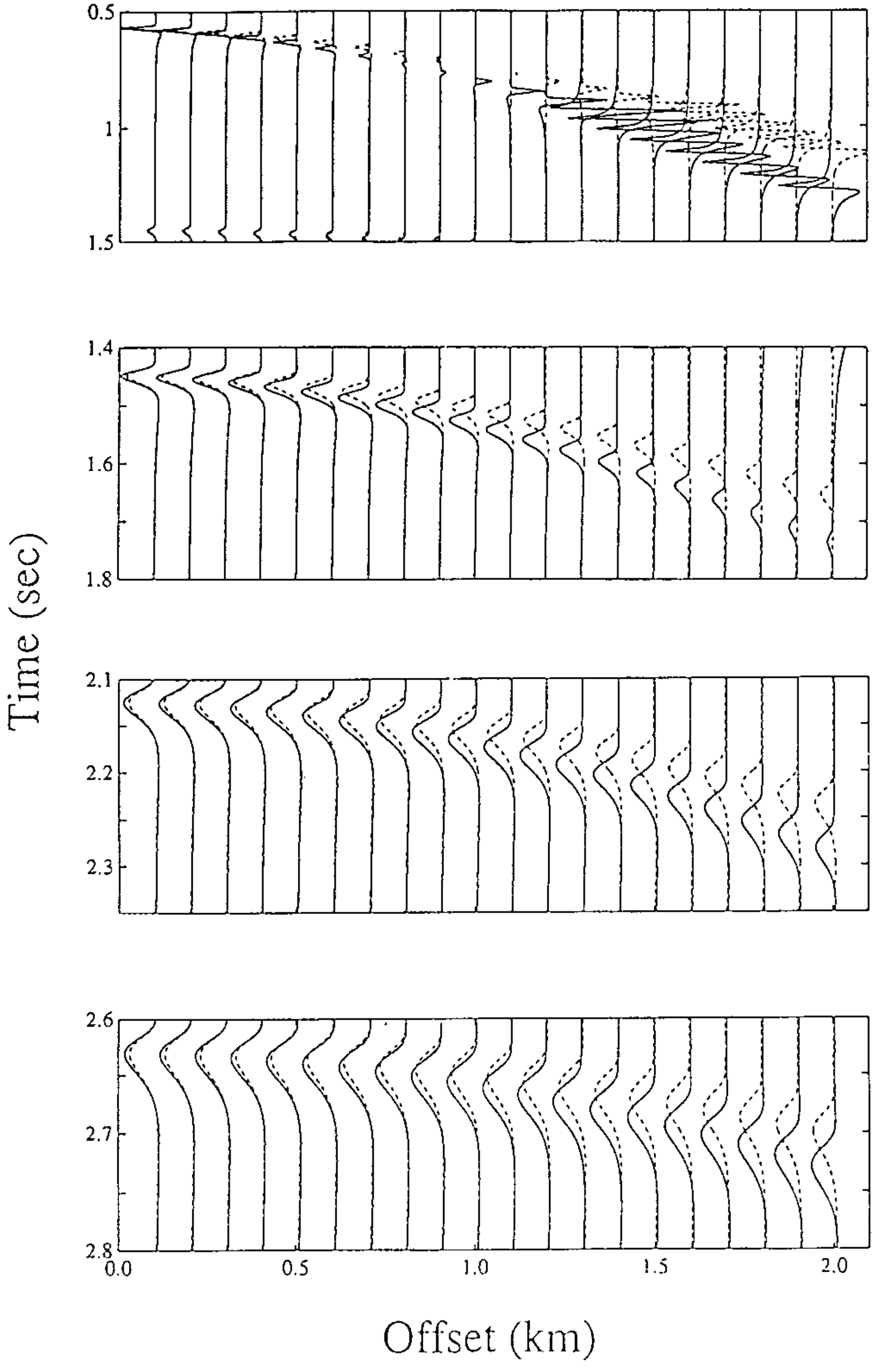

Figure 5. Ray-synthetic seismograms for the model in TABLE 1. Four reflection events, displayed in different time windows for comparison. The solid line traces are for the isotropic model and the dashed line traces for the TI model.